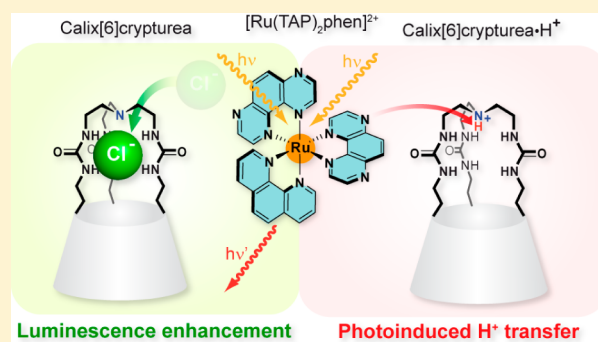


Revisited Photophysics and Photochemistry of a Ru-TAP Complex Using Chloride Ions and a Calix[6]crypturea

Mateusz Rebarz,^{†,§} Lionel Marcélis,^{†,§} Mickaël Menand,[‡] Damien Cornut,[‡] Cécile Moucheron,[†] Ivan Jabin,[‡] and Andrée Kirsch-De Mesmaeker^{*,†}[†]Chimie Organique et Photochimie, Université Libre de Bruxelles, CP 160/08, 50 Avenue Franklin Roosevelt, B-1050 Brussels, Belgium[‡]Laboratoire de Chimie Organique, Université Libre de Bruxelles, CP 160/06, 50 Avenue Franklin Roosevelt, B-1050 Brussels, Belgium

S Supporting Information

ABSTRACT: The effects of the nonprotonated and protonated calix[6]crypturea **1**/**1**[•]H⁺ on the PF₆⁻ and Cl⁻ salts of a luminescent Ru-TAP complex (TAP = 1,4,5,8-tetraazaphenanthrene) were investigated. Thus, the phototriggered basic properties of this complex were examined with **1**[•]H⁺ in acetonitrile (MeCN) and butyronitrile (BuCN). The Ru excited complex was shown to be able to extract a proton from the protonated calixarene, accompanied by a luminescence quenching in both solvents. However, in BuCN, the Cl⁻ salt of the complex exhibited a surprising behavior in the presence of **1**/**1**[•]H⁺. Although an emission decrease was observed with the protonated calixarene, an emission increase was evidenced in the presence of nonprotonated **1**. As the Cl⁻ ions were shown to inhibit the luminescence of the complex in BuCN, this luminescence increase by nonprotonated **1** was attributed to the protection effect of **1** by encapsulation of the Cl⁻ anions into the *tris*-urea binding site. The study of the luminescence lifetimes of the Ru-TAP complex in BuCN as a function of temperature for the PF₆⁻ and Cl⁻ salts in the absence and presence of **1** led to the following conclusions. In BuCN, in contrast to MeCN, in addition to ion pairing, because of the poor solvation of the ions, the luminescent metal-to-ligand charge transfer (³MLCT) state could reach two metal-centered (³MC) states, one of which is in equilibrium with the ³MLCT state during the emission lifetime. The reaction of Cl⁻ with this latter ³MC state would be responsible for the luminescence quenching, in agreement with the formation of photosubstitution products.



■ INTRODUCTION

The photophysics of Ru(II) complexes based on the bpy/phen and bpz/bpym (bpy = 2,2'-bipyridine, bpz = 2,2'-bipyrazine, phen = 1,10-phenanthroline, bpym = 2,2'-bipyrimidine) ligands, has been described and clearly discussed a long time ago.¹⁻⁴ Since then, their proposed photophysical scheme has been adopted as a model by most of the researchers who studied the numerous Ru complexes that have been synthesized during all of those years. Ultrafast spectroscopy with Ru complexes has also been investigated.⁵⁻⁷ Presently, new photophysical experiments carried out in order to examine the photophysics of some Ru complexes are not abundant in the literature, in comparison to the number of new complexes that have been prepared. More recently, the photophysics of Ru complexes used as intercalators of DNA, with DPPZ (dipyrido[3,2-a:2',3'-c]phenazine)⁸⁻¹¹ and PHEHAT (1,10-phenanthroline[5,6-b]1,4,5,8,9,12-hexaazatriphenylene)¹² ligands has been thoroughly investigated. In those cases, the researchers' main motivation was the understanding of the origin of their intriguing behavior as "DNA light-switches". Thus, in addition to the classical metal-to-ligand charge transfer

(³MLCT) and metal-centered (³MC) triplet excited states discussed originally for the Ru(II) complexes, a new type of excited state was evidenced, i.e., a dark nonluminescent state responsible for the interesting properties of these DNA intercalating complexes.

A photophysical study of Ru-TAP complexes (TAP = 1,4,5,8-tetraazaphenanthrene; see Figure 1) was published and compared to the photophysics of the original models with bpy/bpz/bipym ligands.¹³ In a continuous effort for the understanding of the photophysical behavior of the Ru-TAP complexes, specific properties of their excited ³MLCT states, such as their basicity¹⁴ and high oxidation power,¹⁵ were also examined. Those studies led to interesting applications, essentially in aqueous solution with biomolecules.^{15,16}

Very recently, with the objective of developing multivalent systems, Ru-TAP complexes linked to calix[4 and 6]arenes were synthesized and their photophysics was studied.¹⁷ Besides their use as multivalent platforms for biological targets,¹⁸

Received: December 9, 2013

Published: February 17, 2014

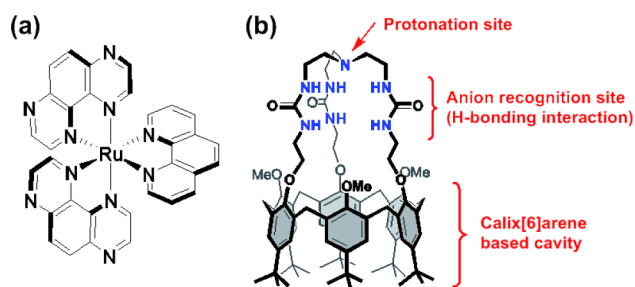


Figure 1. Structure of (a) $[\text{Ru}(\text{TAP})_2(\text{phen})]^{2+}$ and (b) calix[6]crypturea **1**.

calix[*n*]arenes are fascinating concave macrocyclic compounds that can serve for the elaboration of molecular receptors,¹⁹ sensors,²⁰ biomimetic systems,²¹ etc. In this regard, a new family of calix[6]arenes rigidified by a *tris*-urea cap has been developed recently.^{22–24} It was shown that one of these receptors, i.e., calix[6]crypturea **1** (see Figure 1), can strongly bind neutral molecules or ammonium ions into its hydrophobic cavity through hydrogen bonding and CH– π interactions.²⁵ Moreover, the H-bond donor *tris*-urea cap behaves as a particularly efficient binding site for anions. Interestingly, these versatile recognition properties can be modified by protonation of the apical nitrogen atom of the basic cap. In particular, it was shown that calix[6]crypturea **1** can host Cl^- ions with a high affinity in organic solvents ($K_a = 48\,000\text{ M}^{-1}$ in acetonitrile at 243 K),²⁵ which is not the case of its protonated derivative $\mathbf{1}\cdot\text{H}^+$. This acid–base control of the binding properties was exploited notably for guest switching processes. It is noteworthy to mention that such examples of acid–base switching systems based on calixarenes are rare in the literature.^{26–28}

These unique host–guest properties prompted us to investigate the effects of $1/\mathbf{1}\cdot\text{H}^+$ on the photophysical and photochemical behavior of different salts of a TAP complex with phototriggered basic properties. Indeed, the MLCT character of the electronic transition from the Ru center to one of its TAP ligands confers an increased basicity to the relaxed ³MLCT excited state ($\sim 6\text{ p}K_a$ units), which can then deprotonate a proton donor.^{14,29} The study of this light-pulse triggered acid–base reaction in the presence of $\mathbf{1}\cdot\text{H}^+$ could be of special interest since, as mentioned above, the recognition properties of this receptor depend on its protonation state. Because the calixarenes **1** and $\mathbf{1}\cdot\text{H}^+$ are poorly soluble in water, such a study had to be performed in organic solvents. Two organic solvents were chosen: acetonitrile (MeCN) and butyronitrile (BuCN). The first one has a higher dielectric constant and can be hosted by $\mathbf{1}\cdot\text{H}^+$, which is not the case for BuCN.²⁵ As the phototriggered base, we choose the $[\text{Ru}(\text{TAP})_2\text{phen}]^{2+}$ (phen = 1,10-phenanthroline) complex (Figure 1) under the form of PF_6^- or Cl^- salt, because this complex was shown to be much more photostable than $[\text{Ru}(\text{TAP})_3]^{2+}$, at least in aqueous solution.³⁰ Moreover, $[\text{Ru}(\text{TAP})_2\text{phen}]^{2+}$ has a much longer ³MLCT emission lifetime, which should facilitate the acid–base reaction in the excited state.

Herein, we describe the behavior of $[\text{Ru}(\text{TAP})_2\text{phen}]^{2+}$ (as PF_6^- and Cl^- salts) under illumination in the presence of calix[6]crypturea **1** and its protonated form $\mathbf{1}\cdot\text{H}^+$. The objective of this study is 2-fold: exploration of the possibility of phototriggering the recognition properties of the calixarene receptor using this Ru-TAP complex and, conversely, investigation of the photochemical properties of the complex

in organic solvents, thanks to the encapsulation of specific anions by the calixarene.

EXPERIMENTAL SECTION

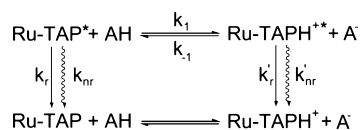
1. Materials. $[\text{Ru}(\text{TAP})_2(\text{phen})]\text{Cl}_2$ was synthesized and purified as reported previously.^{31,32} The corresponding PF_6^- salt was obtained as usual by adding an aqueous solution of KPF_6 to the Cl^- salt of the complex, followed by filtration of the precipitate. Calix[6]crypturea (**1**) was synthesized²² and characterized²⁵ by ¹H NMR spectroscopy and electrospray mass spectrometry (ESI-MS), as described elsewhere. To obtain the protonated derivative $\mathbf{1}\cdot\text{H}^+$, **1** (50.5 mg, 36.9 μmol) was dissolved in CH_3CN (1 mL) and CH_2Cl_2 (2 mL, previously filtered over basic alumina to remove residual HCl). Para-toluenesulfonic acid monohydrate (6.1 mg, 32.1 μmol) (PTSA) was added gradually at room temperature and the protonation of calix[6]crypturea **1** was monitored by ¹H NMR spectroscopy to avoid an excess of acid PTSA in the solution (see Figure S1 in the Supporting Information (SI)). The measurements were performed with a 600 MHz Varian spectrometer and the chemical shifts were expressed in ppm with traces of residual solvent used as internal standard. The final percentage of protonation was estimated to be $86 \pm 5\%$ by integration of appropriate ¹H NMR signals. The solvent then was evaporated and the product was dissolved in butyronitrile (spectroscopic grade) to obtain a stock solution. Since PTSA was used for the protonation procedure, the $\mathbf{1}\cdot\text{H}^+$ samples contained some para-toluenesulfonate (pTSA^-). Therefore, it was checked whether the luminescence of the Ru complex could be perturbed by the presence of pTSA^- (caused, for example, by a quenching by electron transfer from pTSA^-), but this was not the case. Furthermore, as $86\% \pm 5\%$ of protonation of **1** was reached, it was tested whether the nonprotonated calix[6]crypturea **1** (ca. $14\% \pm 5\%$) could behave as quencher of the complex luminescence. This was not the case in butyronitrile. However, in acetonitrile, a slight quenching by nonprotonated **1** was observed (vide infra).³³

2. Methods. The luminescence lifetimes were measured by the time-correlated single photon counting (TC-SPC) technique with the Edinburgh Instruments FL900 spectrometer equipped with a laser diode ($\lambda = 439\text{ nm}$, pulse = 100 ps). The samples were thermostatted at $20 \pm 2\text{ }^\circ\text{C}$ with a Haake Model NB22 temperature controller. The data were collected by a multichannel analyzer (2048 channels) with a number of counts in the first channel ($t = 0$) at the minimum equal to 10^4 . The resulting decays were deconvoluted for the instrumental response and fitted to the exponential functions using the original manufacturer software package (Edinburgh Instruments). The reduced χ^2 , weighted residuals and autocorrelation function were employed to judge the quality of the fits. The steady-state luminescence measurements were performed on a Shimadzu Model RF5001PC spectrofluorometer. For the luminescence lifetime measurements as a function of temperature, the pulsed excitation source was a pulsed laser Nd:YAG Q-switched laser (Continuum, Inc.) frequency-tripled (355 nm) coupled with an optical parametric oscillator (Continuum, Inc.) covering the wavelength region of 410–2300 nm with a maximum pulse energy of 10–120 mJ, depending on the wavelength. The emission was detected perpendicularly by a photomultiplier (Model R928, Hamamatsu). The signal was recorded with a digital oscilloscope (HP Model 54200A), connected through the IEEE488 interface to a personal computer, and was averaged over at least 16 shots. The emission wavelength was selected via a grating Czerny–Turner monochromator (Spectra Pro 2300i, Acton Research Corp.). An Oxford Instruments Model DN 1704 nitrogen cryostat was used to control the temperature. Absorption measurements were carried out using a spectrophotometer (Perkin–Elmer, Model Lambda 35). For the experiments under steady-state illumination, a 150 W Xe arc lamp (Applied Photophysics) (for room-temperature measurements) or a 500 W Xe arc lamp (Oriel) (for variable-temperature experiments) were used.

RESULTS AND DISCUSSION

1. Quenching of Excited $[\text{Ru}(\text{TAP})_2\text{phen}]^{2+}$ as PF_6^- Salt by Protonated Calixarene 1^+H^+ in BuCN and MeCN. As mentioned in the Introduction, one of the goals of this work was to test whether the deprotonation of the protonated calixarene 1^+H^+ can be triggered under illumination of a photosensitizer such as a Ru-TAP complex. Therefore, in order to verify that $[\text{Ru}(\text{TAP})_2\text{phen}]^{2+}$ is able to behave as a base in its $^3\text{MLCT}$ excited state in the presence of the protonated calix 1^+H^+ (more or less 86% protonation; see the Experimental Section), we measured the emission intensities of the complex in the PF_6^- salt as a function of the 1^+H^+ concentration in BuCN and MeCN. Previous studies^{14,29} have shown that the acid–base equilibrium (Scheme 1) between an excited Ru-TAP

Scheme 1. Acid–Base Equilibrium in the Excited State, Where $(k'_r + k'_{nr})^{-1}$ and $(k_r + k_{nr})^{-1}$ are the Lifetimes of the Protonated and Nonprotonated Excited Complex, Respectively



complex in its $^3\text{MLCT}$ state (base) and an acid (AH), cannot be established during the time scale of the excited-state lifetime; the protonated excited Ru-TAP complex deactivates too rapidly to the ground state $(k'_r + k'_{nr})^{-1}$, compared to its deprotonation rate (k_{-1}) for regenerating the nonprotonated excited complex (thus, $(k'_r + k'_{nr}) \gg k_{-1}$). Therefore, a real thermodynamic $\text{p}K_a$ value of the excited state cannot be determined: only an apparent $\text{p}K_a$ value is accessible.

Because of this lack of thermodynamic equilibrium, the quenching of luminescence of the basic form of excited $[\text{Ru}(\text{TAP})_2\text{phen}]^{2+}$ should obey a linear Stern–Volmer relation.¹⁴ This is indeed the case with $[\text{Ru}(\text{TAP})_2\text{phen}](\text{PF}_6)_2$ with increasing concentrations of 1^+H^+ in butyronitrile and acetonitrile (see Figure 2). Similar values of the quenching rate constants ($k_q = 3.0 \times 10^8 \text{ M}^{-1} \text{ s}^{-1}$ for BuCN and $2.7 \times 10^8 \text{ M}^{-1} \text{ s}^{-1}$ for MeCN) are obtained in both solvents, thus independent of the fact that MeCN can be hosted in 1^+H^+ , whereas it is not possible for BuCN.

From these experiments, we can conclude that a proton transfer is possible from the protonated calix[6]crypturea 1^+H^+ to excited $[\text{Ru}(\text{TAP})_2\text{phen}]^{2+}$ as PF_6^- salt in both butyronitrile and acetonitrile. However, it is noted that the k_q values are rather low for a proton transfer. In addition to the incomplete protonation of **1**, this can be attributed to the fact that the reaction takes place in an organic solvent.

2. Quenching of Excited $[\text{Ru}(\text{TAP})_2\text{phen}]^{2+}$ as Cl^- Salt by Protonated Calixarene 1^+H^+ in BuCN and MeCN. While the behavior of excited $[\text{Ru}(\text{TAP})_2\text{phen}]^{2+}$ as PF_6^- salt with increasing 1^+H^+ concentrations is similar in BuCN and MeCN (Figure 2), there is a solvent dependence with the Cl^- counterions. In MeCN, the k_q value is comparable to that obtained for the PF_6^- salt ($k_q = 3.9 \times 10^8 \text{ M}^{-1} \text{ s}^{-1}$, Figure 3a). In contrast, the emission of excited $[\text{Ru}(\text{TAP})_2\text{phen}]\text{Cl}_2$ in BuCN as a function of 1^+H^+ concentrations cannot be plotted in the form of a Stern–Volmer relation. Instead of observing a luminescence quenching, the emission intensity increases to reach a maximum at $\sim 1.25 \times 10^{-4} \text{ M}$ in 1^+H^+ , and decreases for higher 1^+H^+ concentrations.

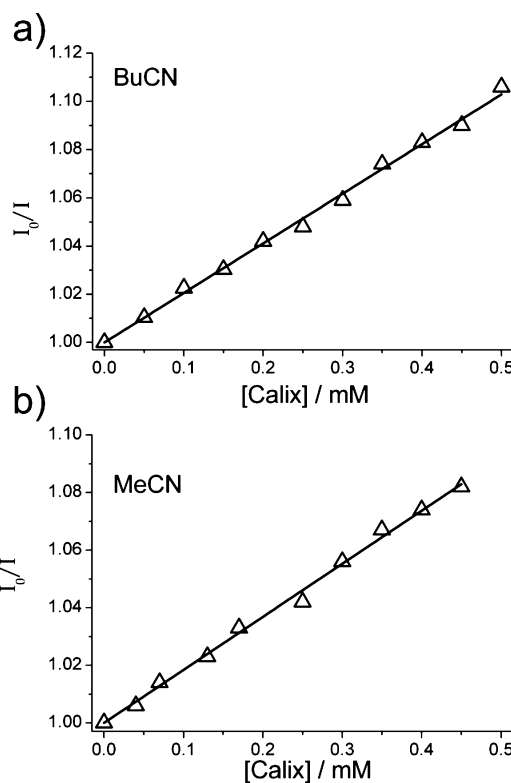


Figure 2. Stern–Volmer plots in intensity in (a) butyronitrile and (b) acetonitrile (under air) for $[\text{Ru}(\text{TAP})_2\text{phen}](\text{PF}_6)_2$ quenched by 1^+H^+ . Some experimental problems prevent to obtain precise values for k_q .³³

As mentioned in ref 33, according to ^1H NMR titrations (see Figure S1 in the SI), 1^+H^+ contained $\sim 14\% \pm 5\%$ nonprotonated **1** that might be responsible for the initial increase in emission intensity up to a concentration of $1.25 \times 10^{-4} \text{ M}$ of 1^+H^+ . Indeed, at this stage, the corresponding 14% of **1** (i.e., $1.75 \times 10^{-5} \text{ M}$) is in the same range of magnitude as the concentration of the Cl^- anion (i.e., $2 \times 10^{-5} \text{ M}$) coming from $[\text{Ru}(\text{TAP})_2\text{phen}]\text{Cl}_2$ (i.e., $1 \times 10^{-5} \text{ M}$). Since **1** can host the Cl^- ion,²⁵ the encapsulation of Cl^- would afford efficient protection of the excited complex from a quenching by Cl^- , leading to the increasing luminescence in BuCN. With higher concentrations of 1^+H^+ ($> 1.25 \times 10^{-4} \text{ M}$), the emission intensity decreases, as expected for a luminescence quenching by proton transfer from 1^+H^+ . In conclusion, this variation of the emission intensity as a function of 1^+H^+ (Figure 3b, empty triangles) would represent the result of two antagonistic effects: an increase due to remaining nonprotonated **1** and a decrease due to the quenching by 1^+H^+ . This behavior in Figure 3b points out the experimental problems related to the study of the photoinduced deprotonation of 1^+H^+ by the Ru-TAP complex as Cl^- salt in BuCN; these problems prevented us from performing further studies of this phototriggered process. Moreover, although in MeCN, the quenching by 1^+H^+ looks normal (Figure 2), there is another problem in MeCN which originates also from the incomplete protonation of **1**, i.e., a slight luminescence quenching by **1** probably by electron transfer from **1** to the excited complex.³³

Despite these different problems, the results described in Figure 3b for BuCN are nevertheless interesting and prompted us to examine further the other effect of the calixarene (in this case, in its nonprotonated state); thus, its protection effect of

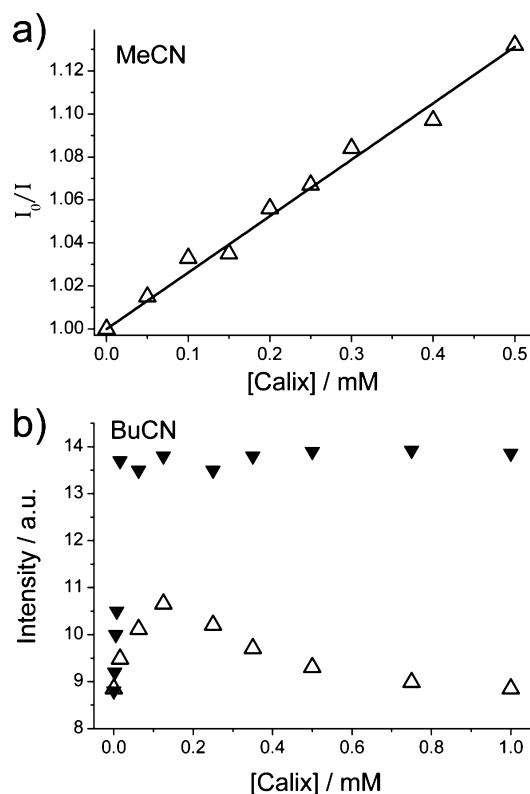


Figure 3. (a) Stern–Volmer plots in intensity in acetonitrile (under air) for $[\text{Ru}(\text{TAP})_2\text{phen}]\text{Cl}_2$ (10^{-5} M) with increasing $1\cdot\text{H}^+$ concentrations. The quenching constant (k_q) should probably be higher (cf Figure 2, not 100% protonation). (b) Luminescence intensity of $[\text{Ru}(\text{TAP})_2\text{phen}]\text{Cl}_2$ (10^{-5} M) as a function of $1\cdot\text{H}^+$ concentrations (not 100% protonation) (empty triangles, Δ) in BuCN and luminescence intensity of $[\text{Ru}(\text{TAP})_2\text{phen}]\text{Cl}_2$ (10^{-5} M) as a function of nonprotonated **1** in BuCN (data symbolized by solid inverted triangles, \blacktriangledown).

the excited-state emission from a Cl^- quenching. This protection is probably due as suggested above, to an encapsulation of the Cl^- anions by the calixarene.

In agreement with this hypothesis, upon the addition of 2×10^{-5} M of nonprotonated **1** to a BuCN solution 10^{-5} M in complex as Cl^- salt, the emission intensity increases with the first additions of **1** and reaches a plateau value when the total amount of Cl^- ions is encapsulated by **1** (Figure 3b, full triangles). This protection effect by **1** in BuCN can also be observed from the luminescence lifetimes (Table 1) that increase until a concentration of **1** quasi equal to twice that of

Table 1. Luminescence Lifetimes of Excited $[\text{Ru}(\text{TAP})_2\text{phen}]\text{Cl}_2$ (10^{-5} M) in the Presence of Increasing Concentrations of **1** in BuCN (under Air)^a

1 [M]	τ [ns]
0	445
2.5×10^{-6}	468
5.0×10^{-6}	489
7.5×10^{-6}	505
1.7×10^{-5}	663
1.1×10^{-4}	671
2.5×10^{-4}	670

^aSee also ref 34. Experimental error is $\sim 5\%$.

the Ru complex (i.e., the concentration of Cl^- counterions) is observed. The constant value reached by the excited-state lifetime (i.e., ~ 670 ns) corresponds (within experimental errors) to the value measured for the excited Ru complex with PF_6^- counterions in BuCN (680 ns, under air) (see also Table S1 in the SI).

Since quenching by Cl^- takes place in the BuCN solvent (dielectric constant of $\epsilon = 22$) and not in the MeCN solvent ($\epsilon = 37.5$) (see Figure S2 in the SI), in which the ions should be more solvated than in BuCN, it is concluded that ion pairing should be present in BuCN.

3. Ion Pairing and Quenching by Cl^- in BuCN. In order to test the presence of ion pairing and, in consequence, the presence of possible static quenching by Cl^- in BuCN, the modification of the absorption spectrum of $[\text{Ru}(\text{TAP})_2\text{phen}](\text{PF}_6)_2$ upon addition of tetrabutyl ammonium chloride (TBACl) first must be examined. The presence of Cl^- clearly affects the absorption spectrum of the complex, which indicates the formation of ion pairs in the ground state (see Figure S3 in the SI) with rather weak absorption changes between 0 and 20 equiv. Next, the Stern–Volmer plots for the luminescence quenching of $[\text{Ru}(\text{TAP})_2\text{phen}](\text{PF}_6)_2$ by TBACl in BuCN in emission intensities and lifetimes have been determined. As shown in Figures 4a and Figure S3 in the SI, the changes in emission are very important and not accompanied by a shift of λ_{max} of emission. The upward curvature of the Stern–Volmer plot for the I_0/I data is characteristic of systems where both

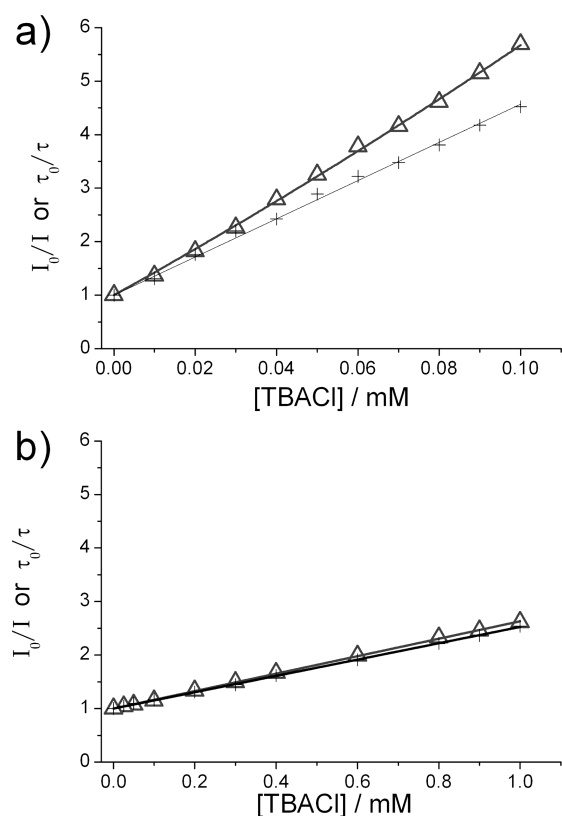


Figure 4. Stern–Volmer plots for $[\text{Ru}(\text{TAP})_2\text{phen}](\text{PF}_6)_2$ (10^{-5} M) in BuCN with increasing TBACl concentrations (under air) (a) in luminescence intensity (triangles, Δ) and excited-state lifetime (crosses, $+$) and (b) same as that in panel (a), but with 100 mM tetrabutylammonium hexafluorophosphate (TBAPF₆).

static and dynamic quenching occurs and can be described by the modified Stern–Volmer equation:³⁵

$$\frac{I_0}{I} = 1 + (K_{SV} + K_{ass})[Q] + (K_{SV} \times K_{ass})[Q]^2 \quad (1)$$

where $[Q]$ is the concentration of quencher (Cl^-), K_{ass} is the equilibrium constant for the formation of ion pairs (Ru complex with Cl^-), and K_{SV} is the Stern–Volmer constant. From the Stern–Volmer relation in τ_0/τ , which does not include static quenching ($\tau_0/\tau = 1 + k_q\tau_0[Q]$) (see Figure 4a), the value of K_{SV} is determined:

$$K_{SV} = k_q\tau_0 = 36\,720 \text{ M}^{-1}$$

With the excited-state lifetime of the complex as PF_6^- salt in BuCN ($\tau = 680$ ns, under air), the dynamic quenching rate constant (k_q) can be obtained and is equal to $5.4 \times 10^{10} \text{ M}^{-1} \text{ s}^{-1}$. This rather high value of k_q contains not only a contribution of diffusion but also electrostatic interaction (between the positively charged Ru complex and the negatively charged Cl^- anion). Therefore, to examine the influence of the ionic strength on the quenching rate constant k_q , the same Stern–Volmer experiments (in I_0/I and τ_0/τ) have been carried out with different constant concentrations of tetrabutylammonium hexafluorophosphate (TBAPF₆) (see Table 2). A same

Table 2. Quenching Rate Constants (k_q) and Equilibrium Constants (K_{ass}) Determined from Stern–Volmer Plots (I_0/I) from eq 1, in the Presence of Different Constant Concentrations of TBAPF₆

$[\text{TBA}^+ \text{PF}_6^-] \text{ (M)}$	$k_q \text{ dyn. (M}^{-1} \text{ s}^{-1}\text{)}$	$K_{ass} \text{ (M}^{-1}\text{)}$
0	5.40×10^{10}	2280
10^{-3}	2.70×10^{10}	505
10^{-2}	1.00×10^{10}	
10^{-1}	0.24×10^{10}	

straight line in τ_0/τ and I_0/I was obtained with 100 mM TBAPF₆ (see Figure 4b). When the ion pairing and electrostatic interaction no longer interfere, the k_q value ($2.4 \times 10^9 \text{ M}^{-1} \text{ s}^{-1}$) corresponds to a diffusion-limited process and the static quenching has vanished. By fitting the data of emission intensity (I_0/I) in the absence (Figure 4a) and in the presence of up to 100 mM TBAPF₆ (Figure 4b) to eq 1, and using a K_{SV} constant determined from the τ_0/τ relation, K_{ass} values of 2280 M^{-1} and 505 M^{-1} , are found (see Table 2). This ion-pairing association is rather weak in comparison with that between other Ru complexes and iodide³⁶ and chloride;³⁷ however, in those cases, the measurements were performed in a less-polar solvent (i.e., CH_2Cl_2).

4. Possible Origin of Luminescence Quenching by Cl^- in BuCN. **4.1. Quenching by Electron Transfer (ET).** A first possible origin of luminescence quenching by Cl^- would be an electron transfer process (ET) from Cl^- to the excited complex. As mentioned above, such a photoinduced ET does not take place in MeCN, since no quenching by Cl^- was detected in that solvent; it could nevertheless take place in BuCN. According to the redox potentials, it is indeed thermodynamically possible ($\Delta G^0 = -0.01 \text{ eV}$).³⁸ Therefore, the presence of an ET was tested by pulsed-laser experiments with the complex as PF_6^- salt without (data not shown) or with added TBACl in BuCN (see Figures S4 and S5 in the SI). Under these conditions, the characteristic signatures of formation of (i) the transient reduced complex (i.e., a clear transient absorption at ~ 500

nm),¹⁵ and (ii) the oxidation product of Cl^- (i.e., $\text{Cl}_2^{\bullet -}$ at 360 nm, after reaction of radical chloride with Cl^-)³⁹ could not be detected. The only detectable transient was the excited ³MLCT state (see Figure S4 in the SI) with a maximum bleaching at ~ 425 nm and emission at ~ 625 nm, with a lifetime on the order of 20 ns. A permanent absorption could nevertheless be observed at ~ 500 nm (see Figure S5 in the SI), which would suggest that TAP dechelation products, absorbing in this spectral region, are formed. Thus, no strong arguments in favor of an ET process exist, which would explain an emission quenching by Cl^- .

4.2. Reaction of Cl^- with the ³MC Excited State, Generating Quenching of the ³MLCT Emission. Another possibility for the origin of the important luminescence quenching as proposed in the past^{3,13} would be the following. It is generally accepted that an important mode of nonradiative deactivation of the Ru complexes ³MLCT states involves a thermally activated pathway from the ³MLCT state to an excited metal-centered state ³MC, which is nonluminescent and responsible for ligand loss processes.^{12,40} However, for $[\text{Ru}(\text{TAP})_2\text{phen}]\text{Cl}_2$ or $[\text{Ru}(\text{TAP})_2\text{phen}](\text{PF}_6)_2$ in water, no photodechelation product at all was observed,³⁰ therefore, it was assumed that, in aqueous solution, there is no contribution of the ³MC state. In BuCN, a much less polar solvent, the ³MLCT state is not as well-solvated as in water, so that its energy level is less stabilized (see Table S1 in the SI for further λ_{max} data regarding the emissions in water, MeCN, and BuCN) and may be closer or even very close to the ³MC state level. Therefore, in that case, activation to the ³MC state and a loss of ligand become possible at room temperature. However, the reaction with Cl^- anions concerns the ³MC state and an explanation must be provided for the luminescence quenching (dynamic and static) of the ³MLCT state. If the Cl^- anions attack the ³MC state and “kill” it into a final dechelated product, this should not give rise to a ³MLCT luminescence quenching except if the two triplets, ³MLCT and ³MC, are in fast equilibrium.^{13,41} We have thus tested this possibility by two types of experiments: (i) measurements of emission lifetimes as a function of temperature and the influence of calixarene **1** at the different temperatures, and (ii) detection of photoproducts at a few key temperatures in the presence and absence of Cl^- and calixarene **1**.

5. Study of the ³MLCT Emission Lifetime, as a Function of Temperature. **5.1. In MeCN, a Classical Behavior.** In order to have a reference for the excited-state lifetime behavior as a function of temperature, without the effect of Cl^- anions or ion pairing, measurements have first been performed in MeCN. As shown in Figure 5, in the temperature domain of 340–240 K, there is indeed no influence of Cl^- on the luminescence lifetimes. Two temperature domains can be distinguished: (i) from 340 K to 270 K, the luminescence lifetime increases for decreasing temperatures, (ii) from 270 K to lower temperatures, a plateau value is reached. The increase of lifetime is due to the well-known temperature dependence of the activation process from the ³MLCT to the ³MC state. Despite the fact that the ³MC state is reached and can be attacked by Cl^- , there is no influence on the luminescent lifetime, simply because the ³MC state, during its lifetime, does not go back to the ³MLCT state. From 270 K to lower temperatures, the ³MC state can no longer be thermally populated and the lifetime remains constant. This dependence of lifetime with temperature can be described by eq 2 and by the scheme in Figure 6a, where A_{MC} stands for the pre-

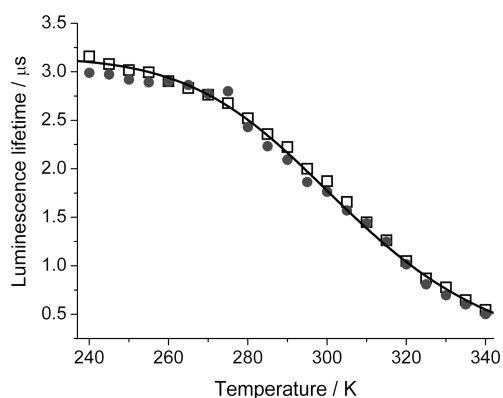


Figure 5. Luminescence lifetimes of $[\text{Ru}(\text{TAP})_2\text{phen}](\text{PF}_6)_2$ (squares, \square) and $[\text{Ru}(\text{TAP})_2\text{phen}]\text{Cl}_2$ (circles, \bullet) in MeCN as a function of temperature from 340 K to 240 K (under argon) and calculated curve according to eq 2 (solid line). Experimental error = $\pm 5\%$.

exponential factor of the rate constant for the activation process and E_{MC}^\ddagger represents the activation energy from the $^3\text{MLCT}$ to the ^3MC state.

$$\tau^{-1} = k_r + k_{\text{nr}} + A_{\text{MC}} \exp\left(-\frac{E_{\text{MC}}^\ddagger}{RT}\right) \quad (2)$$

The parametric adjustment of the experimental data of Figure 5 to eq 2 leads to the simulated curve (Figure 5) and the calculated parameters collected in Table 3 (those for $[\text{Ru}(\text{bpy})_3]^{2+}$ are given for comparison purposes); they will be compared with those calculated for BuCN (vide infra). From the data in MeCN, it is concluded that an activation energy of $E_{\text{MC}}^\ddagger > 3000 \text{ cm}^{-1}$ corresponds to an irreversible process from the $^3\text{MLCT}$ to the ^3MC state. This corresponds to a “classical” behavior of the emission lifetime with temperature.

5.2. In BuCN. In BuCN, which allows the investigations until 180 K (before matrix formation), the dependence of the luminescence lifetime with temperature is different from that in MeCN. Figure 7a shows the curves for the PF_6^- and Cl^- counterions and also for each counterion in the presence of **1**.

The most striking observation is the quenching by Cl^- in the absence of **1** in the entire temperature domain, in contrast to

Table 3. Parameters for the Deactivation of the Excited $^3\text{MLCT}$ State of $[\text{Ru}(\text{TAP})_2\text{phen}]^{2+}$ in MeCN Determined by Simulation of the Emission Lifetimes, as a Function of Temperature According to eq 2^a

complex	$k_r + k_{\text{nr}} (\times 10^5 \text{ s}^{-1})$	$A_{\text{MC}} (\times 10^{13} \text{ s}^{-1})$	$E_{\text{MC}}^\ddagger (\text{cm}^{-1})$
$[\text{Ru}(\text{TAP})_2\text{phen}]^{2+}$	3.31	1.1	3700
$[\text{Ru}(\text{bpy})_3]^{2+ 13}$	5.57	5.8	3800

^aThe values obtained for $[\text{Ru}(\text{bpy})_3]^{2+}$ are given for comparison purposes. Estimated errors: for E_{MC}^\ddagger , $\pm 50 \text{ cm}^{-1}$; for $(k_r + k_{\text{nr}})$, $\pm 10\%$; and for A_{MC} , $\pm 20\%$.

the MeCN case. In the presence of the calixarene **1**, the Cl^- effect is inhibited. Another difference, compared to the MeCN case, is the absence of plateau reached by the emission lifetimes values in the lower temperature domain (see Figure 7b). In order to simulate these new data by curve fitting as performed for the dependence in Figure 5 for MeCN, and in order to evidence these temperature dependences more clearly, the data points only for the PF_6^- and Cl^- salts have been considered for the curve fitting in Figure 7b. From that figure, two different types of dependences on temperature can be distinguished, at least in the absence of Cl^- : (i) one in the high-temperature (HT) domain (Figure 7b) from 310 K to 260 K, whose temperature dependence is comparable to that in MeCN, and (ii) another in the low-temperature (LT) domain from 260 K to 190 K, with a less important temperature dependence than in the HT domain. This behavior suggests that, in BuCN, in contrast to MeCN, two thermally activated processes toward two ^3MC states at lower and higher energy would contribute to the observed emission. Moreover, as shown in Figure 7, the temperature dependences of these two activation processes are very much affected by the presence of Cl^- . Indeed, the lifetimes are not only shorter over the entire temperature domain, as mentioned above, but the temperature dependence is also weaker.

To explain these behaviors, the following scheme is proposed (Figure 6). Since it would be logical that the two ^3MC states, at higher and lower energy, would remain approximately at their same energy levels in the absence or presence of Cl^- , these two activation processes should also be present with Cl^- . Moreover, one of them should be reversible in the entire temperature domain to explain the Cl^- effect on the $^3\text{MLCT}$ emission.

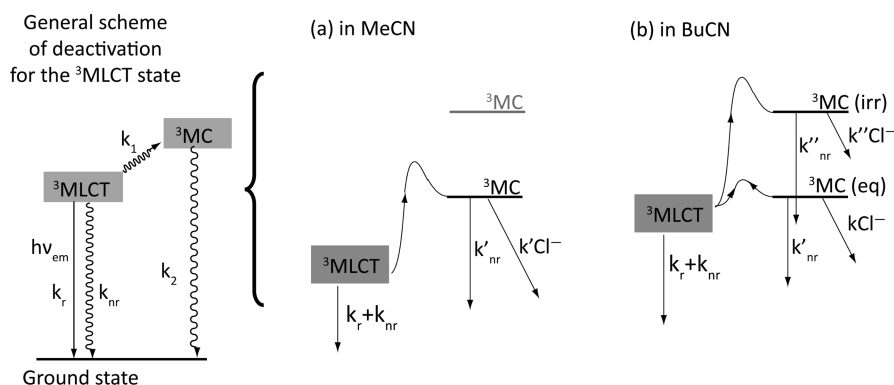


Figure 6. General photochemical scheme for $[\text{Ru}(\text{TAP})_2\text{phen}]^{2+}$ (a) in MeCN and (b) in BuCN. In this figure, it is assumed that the energy levels of the ^3MC states are much less affected by the change of solvent from MeCN to BuCN than the $^3\text{MLCT}$ states, which include an electron transfer to a ligand. k_{nr}' and k_{nr}'' are the radiationless deactivations of the first and second ^3MC state, respectively; $k'\text{Cl}^-$, $k\text{Cl}^-$, and $k''\text{Cl}^-$ represent the reaction of ^3MC with Cl^- which, respectively, does not affect the $^3\text{MLCT}$ emission (irreversible), decreases the $^3\text{MLCT}$ emission (reversible), and does not influence the $^3\text{MLCT}$ emission (irreversible).

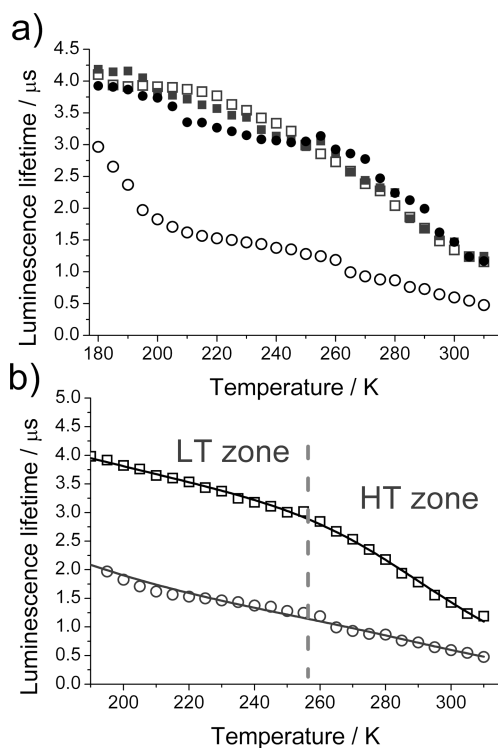


Figure 7. (a) Emission lifetimes (under argon) of [Ru(TAP)₂phen]²⁺ in BuCN with different counterions, PF₆⁻ or Cl⁻, and in the absence or presence of **1** as a function of temperature from 320 K to 180 K (PF₆⁻ salt (open squares, □), PF₆⁻ salt with **1** (full squares, ■), Cl⁻ salt (open circles, ○), and Cl⁻ salt with **1** (full circles, ●)). (b) Emission lifetimes of [Ru(TAP)₂phen]²⁺ in BuCN (squares for the PF₆⁻ salt and circles for the Cl⁻ salt) as described in panel (a). The calculated curves from eq 4 are represented by the solid lines. The experimental data below 190 K in the presence of Cl⁻ have been omitted for the simulation; the increase of lifetime observed in this temperature region could be due to an increase of viscosity of the solvent, which would affect the quenching process by Cl⁻ (*k*Cl⁻, decrease of diffusion quenching). Experimental error = ±5%.

Therefore, it is proposed that at least the activation to the lower ³MC state would correspond to a reversible process (Figure 6b for BuCN). The luminescence lifetimes in the absence or presence of Cl⁻ should thus be expressed by two different temperature-dependent terms: one for an irreversible activation as in MeCN (eq 2), and one for a reversible activation (eq 3) (with steady-state approximation on the ³MC state, as proposed in the previous literature).^{1,3} In the term for the reversible process (eq 3),

$$\tau^{-1} = k_r + k_{nr} + k_2 \exp\left(-\frac{\Delta E_{\text{MLCT-MC}}}{RT}\right) \quad (3)$$

*k*₂ corresponds to the rate constant of deactivation of the lower ³MC state (*k*₂ = *k*'_{nr} + *k*Cl⁻ with *k*'_{nr} = radiationless deactivation of the lower ³MC state and *k*Cl⁻ = quenching term (dynamic and static), which depends on the Cl⁻ concentration); Δ*E*_{MLCT-MC} is the energy difference between the ³MLCT and the ³MC states in equilibrium. The inverse of the luminescence lifetime in the entire temperature domain, without or with Cl⁻, can thus be expressed as

$$\tau^{-1} = k_r + k_{nr} + A_{\text{MC}} \exp\left(-\frac{E_{\text{MC}}^{\#}}{RT}\right) + k_2 \exp\left(-\frac{\Delta E_{\text{MLCT-MC}}}{RT}\right) \quad (4)$$

The adjustment of the experimental data to eq 4 (without and with Cl⁻), gives the values for the different parameters that are collected in Table 4 (calculated curves in Figure 7b). From

Table 4. Parameters of Deactivation of the Excited ³MLCT State of [Ru(TAP)₂phen]²⁺ in BuCN Determined by Parametric Adjustment of the Lifetimes Data to eq 4, for the Two Types of Counterion (PF₆⁻ and Cl⁻)^a

[Ru(TAP) ₂ phen] ²⁺	-2PF ₆ ⁻	-2Cl ⁻
<i>k</i> _r + <i>k</i> _{nr} (× 10 ⁵ s ⁻¹)	2.0	2.3
<i>A</i> _{MC} (× 10 ¹³ s ⁻¹)	1.0	1.3
<i>E</i> _{MC} [#] (cm ⁻¹)	3120	3053
<i>k</i> ₂ (10 ⁵ s ⁻¹)	12	76
Δ <i>E</i> _{MLCT-MC} (cm ⁻¹)	417	454

^aEstimated errors: for *E*_{MC}[#] and Δ*E*_{MLCT-MC} ±50 cm⁻¹; for (*k*_r + *k*_{nr}), ±10%; and for *A*_{MC} and *k*₂, ±20%.

the data of Table 4, the striking observation is the fact that the value of *k*₂ is, of course, much higher in the presence of Cl⁻, which explains the weaker dependence on temperature of the curve with Cl⁻. Indeed, with Cl⁻ the contribution of the second exponential term in eq 4 becomes more important (via the Cl⁻ concentration) than the contribution of this same exponential in the absence of Cl⁻, resulting thus into a weaker dependence of the emission lifetime with temperature. Moreover, an activation energy of *E*_{MC}[#] > 3000 cm⁻¹ is found for the first exponential term (without and with Cl⁻), which is in agreement with an irreversible process as obtained for the MeCN case (Table 3).

In conclusion, in BuCN as depicted in Figure 6b, two ³MC states would play a role: a higher one, which would not be in equilibrium with the ³MLCT state, thus not affecting the ³MLCT luminescence lifetime, and a lower one, in equilibrium with the ³MLCT state and affecting the ³MLCT luminescence lifetime, and this in the entire temperature domain. Once the higher ³MC state would be populated, it can react with Cl⁻ (*k*'Cl⁻). Moreover, trapping of this species by Cl⁻ should not affect the luminescence lifetime but could give rise to photoproducts. By populating the lower ³MC state, the emission lifetime drops with Cl⁻ via the equilibrium and photoproducts should also be observed in the entire temperature domain.

6. Spectroscopic Detection of Photodechelation Products in the HT and LT Domains in MeCN and BuCN. On the basis of the scheme proposed in Figure 6 resulting from consideration of the different data, the occurrence of photoproducts should depend on the temperature, solvent, and presence of Cl⁻.

In MeCN, since the ³MLCT state is well-solvated and thus well-stabilized, only one ³MC state should be thermally accessible and not in equilibrium with the ³MLCT state, since there is no influence on the emission lifetime (Figure 6a). Nevertheless, photoproducts should be observed from the ³MC state in the HT domain. As detected by changes of the absorption spectra after illumination, this is indeed the case (Figure 8a). In contrast, at 260 K, temperature at which a plateau of lifetime values is reached, no photoproduct is detected (see Figure 8b).

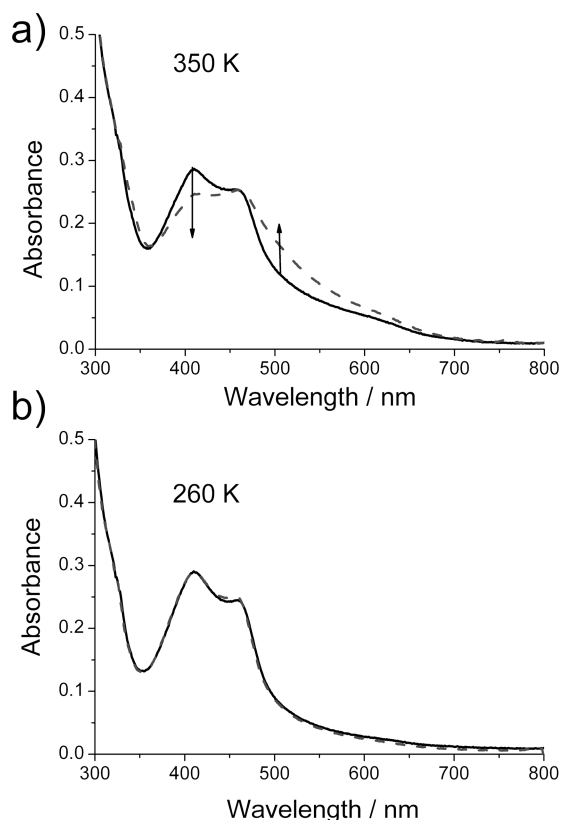


Figure 8. Evolution of the absorption spectra of $[\text{Ru}(\text{TAP})_2\text{phen}]\text{Cl}_2$ in MeCN (a) at 350 K and (b) at 260 K (under argon) after 15 min of irradiation (500 W Xe lamp). The arrows indicate the direction of change after illumination.

In BuCN, as shown in Figure 9, photodechelation occurs in the entire temperature domain, even at 180 K. This contrasts with the illumination in MeCN as the solvent. In conclusion, the examination of the occurrence of photoproducts in MeCN and BuCN at two different temperatures is in agreement with the general photochemical scheme proposed in Figure 6.

7. Effects of the Addition of 1 at Room Temperature on Photodechelation Products in BuCN. Figure 10 shows at room temperature in BuCN, the different evolutions of the absorption spectra according to the counterions and the presence of **1**. With Cl^- as counterions (see Figure 10b), there is a bleaching of the $^3\text{MLCT}$ absorption band (400–460 nm) and occurrence of a new red-shifted band at ~ 500 nm, typical of ligand substitution by Cl^- , as observed for the Cl^- salt in Figures 8 and 9.^{13,42,43} Interestingly, the illumination of the Ru complex in the form of chloride salt but in the presence of the calixarene **1** (Figure 10d) gives rise to different photoproducts probably from photosubstitution of the ligand by BuCN molecules. Indeed, the irradiation of $[\text{Ru}(\text{TAP})_2\text{phen}]^{2+}$ as PF_6^- salt in the absence or presence of **1** (see Figures 10a and 10c) exhibits the same absorption changes as the Cl^- salt with **1** (see Figure 10d). In conclusion, when Cl^- is trapped into the *tris*-urea binding site of the calixarene, the same photoproduct as with the PF_6^- salt of the complex is detected spectroscopically in BuCN.

CONCLUSION

The results presented in this work show that the protonated calixarene $\mathbf{1}\cdot\text{H}^+$ can behave as an acid versus the excited Ru complex in BuCN and MeCN. The quenching rate constants

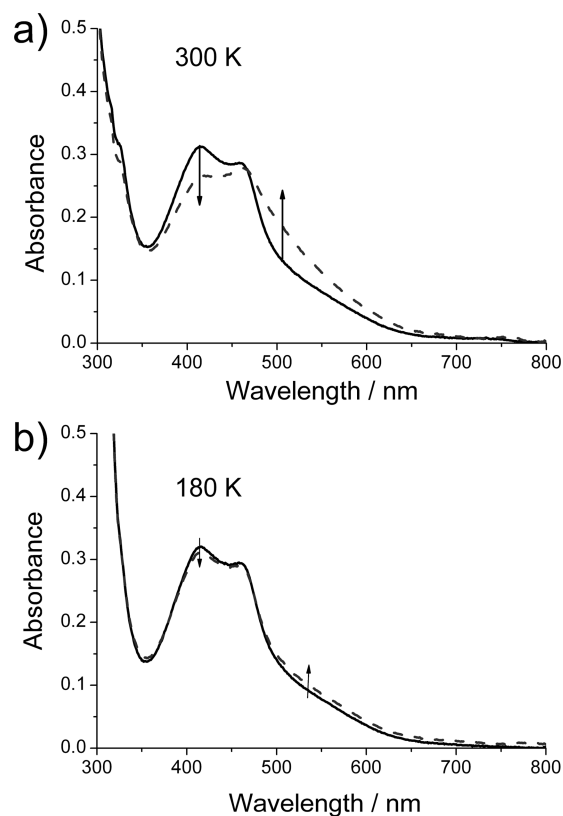


Figure 9. Evolution of the absorption spectra of $[\text{Ru}(\text{TAP})_2\text{phen}]\text{Cl}_2$ in BuCN (a) at 300 K and at (b) 180 K (under argon) after 15 min of irradiation (500 W Xe lamp). At 180 K, obviously the photo-substitution by Cl^- is lower, since, in that case, essentially the lower ^3MC state is populated. The arrows indicate the direction of change after illumination.

determined by Stern–Volmer experiments are not diffusion-controlled and are similar in MeCN and BuCN. Such a slow rate is expected when a proton is not transferred via water molecules. With the Cl^- salt in BuCN, no linear Stern–Volmer relationship was observed as a function of the addition of $\mathbf{1}\cdot\text{H}^+$, simply because 100% of **1** was not protonated. Less than 1 equiv of acid was indeed purposely added to **1**, so that protonation of the excited complex by *p*-toluene sulfonic acid itself could be excluded. As explained above,³³ these experimental problems prevented the examination of the photosensitized deprotonation of $\mathbf{1}\cdot\text{H}^+$ in more details. In contrast, the observation of the abnormal behavior of the chloride salt in BuCN in presence of $\mathbf{1}\cdot\text{H}^+$ motivated us to study the effect of Cl^- on the luminescence of $[\text{Ru}(\text{TAP})_2\text{phen}]^{2+}$ in BuCN by comparison with that in MeCN. As shown in this work, it turned out that calixarene **1** was a useful tool for this study, thanks to its encapsulation properties of the Cl^- ions.

In contrast to MeCN or water, the less-polar BuCN solvent does not solvate the ruthenium complex cation well. This produces ion pairs in the ground state and less stabilization of the excited $^3\text{MLCT}$ state, as indicated by the shift of λ_{max} emission with the solvent (Table S1 in the SI, in which corresponding τ values at room temperature from the previous figures have also been gathered). The ion-pairing process is confirmed by the Cl^- effect on the electronic absorption of the complex.

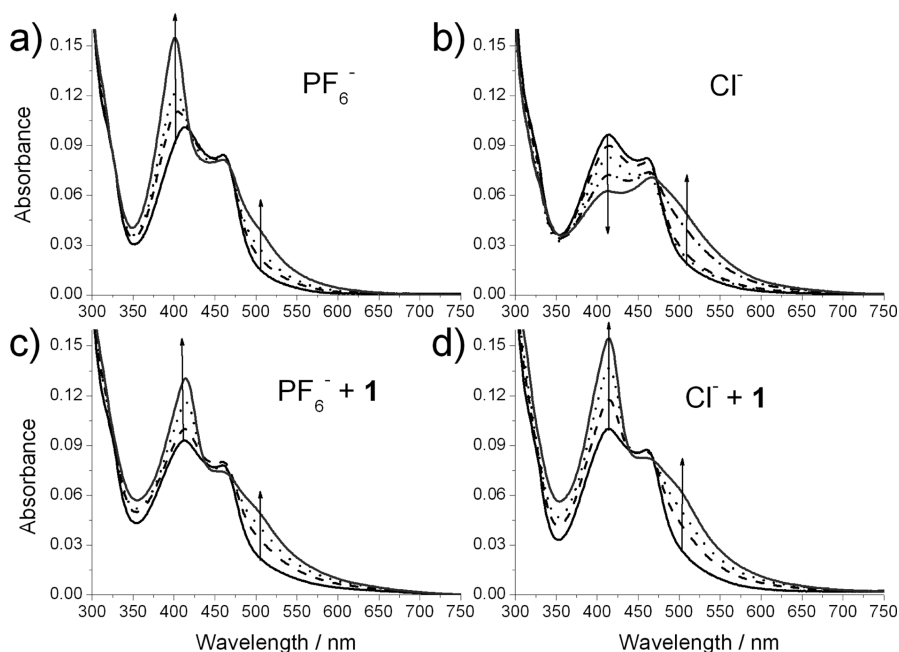


Figure 10. Evolution at room temperature in BuCN of the absorption spectra of $[\text{Ru}(\text{TAP})_2\text{phen}]^{2+}$ (3×10^{-5} M) (a, c) in the PF_6^- form and (b, d) in the Cl^- form for increasing illumination time (0–10 min) in the (a, b) absence and (c, d) presence of **1** in BuCN (argon saturated solution, 500 W Xe lamp irradiation). The arrows indicate the direction of change after illumination.

Moreover, in BuCN, the study of the luminescence lifetimes as a function of temperature fits with a model in which two ^3MC states participate to the deactivation process of the luminescent species, with the lowest ^3MC state in equilibrium with the $^3\text{MLCT}$ state. If we refer now to the results of the Stern–Volmer relations obtained above as a function of $[\text{TBACl}]$ and in the absence of ion pairing, thus, in the presence of 100 mM salt (Figure 4b), we could wonder why, with such an equilibrium $^3\text{MLCT} \rightleftharpoons ^3\text{MC}$ (Figure 6b), the quenching by Cl^- gives rise experimentally to a linear relation. Let us consider first this relation in τ thus determined under pulsed illumination conditions at room temperature. It is reminded that eq 4 for τ^{-1} was obtained with a crude approximation (i.e., a steady state for the ^3MC state, see above). Thus, if we simply use eq 4 for the inverse of the lifetimes, where (i) the second term is the rate constant for the irreversible activation toward the higher ^3MC state and (ii) the third term is $k_2 = (k'_{\text{nr}} + k\text{Cl}^-) \times K (K = k_1/k_{-1})$, the τ/τ_0 ratio gives

$$\frac{\tau_0}{\tau} = 1 + kK\tau_0[\text{Cl}^-] \quad (5)$$

which is thus similar to a Stern–Volmer relation. Consequently, the value of $k_{\text{q,dyn}}$ obtained in Table 2 ($2.4 \times 10^9 \text{ M}^{-1} \text{ s}^{-1}$, in the presence of salt) does not correspond exactly to k , the quenching constant by Cl^- . However, since the equilibrium constant (K) could probably be close to 1, the determined value of $k_{\text{q,dyn}}$ should be close to that of k .

For the Stern–Volmer relation in emission intensity under steady-state illumination conditions, the calculation of $(1/I - 1/I_0)$ without approximation in this case, since the steady-state hypothesis can be assumed safely for the $^3\text{MLCT}$ and ^3MC states, and according to the different kinetic steps described in Figure 6b (see SI for the reactions scheme and calculation), does not result in a linear relation. The function of Cl^- , which is

obtained, could nevertheless lead to a linear relation in first approximation (see the SI), thus, in agreement with our results.

For the other experiments under steady-state illumination, it is also shown from the change of the absorption spectra, that both ^3MC states give rise to photodechelation. It is noted that the lowest ^3MC state as detected here, thus close to the $^3\text{MLCT}$ state, has already been mentioned in a theoretical publication on TAP-complexes by Alary et al.⁴⁴ It must be noted that emission quenching for some Ru complexes with iodide as counteranions in dichloromethane has been previously reported by the Meyer's group.³⁶ Nevertheless, in that case, the authors mention that the "ion pairing with I^- suppresses the photochemistry reported by Van Houten" (i.e., photosubstitution of one ligand) and the luminescence quenching is attributed to an ET process with the $^3\text{MLCT}$ state as demonstrated by pulsed-laser experiments. In the present case, there are no arguments suggesting that an ET process would take place from Cl^- to the $^3\text{MLCT}$ state, despite the fact that with the Ru-TAP complexes an ET reaction could be thermodynamically possible.³⁸ In a more recent work,³⁷ it is shown with other Ru complexes in CH_2Cl_2 as solvent that the emission decrease with Cl^- anions originates from an equilibrium between the solvated ions and the ion pairs. However, in that case, (i) the emission quenching is much less important (30% only) than in the present case, (ii) it is accompanied by a shift of the λ_{max} emission, and (iii) no photoproducts are formed; the behavior is thus quite different from the one observed in this work.

■ ASSOCIATED CONTENT

📄 Supporting Information

NMR spectra of calix[6]crypturea; absorption and luminescence of $[\text{Ru}(\text{TAP})_2\text{phen}]^{2+}$, as a function of chloride concentration in MeCN and BuCN; transient absorption spectra and kinetic decays for $[\text{Ru}(\text{TAP})_2\text{phen}]^{2+}$ under pulsed-laser illumination; λ_{max} of emission; lifetimes and quantum

yields of emission of $[\text{Ru}(\text{TAP})_2\text{phen}]^{2+}$ in H_2O , MeCN ; and BuCN ; kinetic scheme and calculation of I and I_0 under steady-state conditions. This material is available free of charge via the Internet at <http://pubs.acs.org>.

AUTHOR INFORMATION

Corresponding Author

*Tel.: 003226503017. Fax: 003226503018. E-mail: akirsch@ulb.ac.be.

Author Contributions

The manuscript was written through contributions of all authors. All authors have given approval to the final version of the manuscript.

Author Contributions

[§]These authors contributed equally to this work.

Notes

The authors declare no competing financial interest.

ACKNOWLEDGMENTS

The authors thank the Belgian Science Policy (Program No. IAP/PAI, P6/27) and the FRFC-FNRS for financial support. M.R. is grateful to the IAP Program P6/27 for a postdoctoral grant and to The British Council and WBI/FNRS (No. PPS RV03B) for financial support. L.M. is grateful to the FNRS for a Ph.D. grant.

REFERENCES

- (1) Van Houten, J.; Watts, R. J. *J. Am. Chem. Soc.* **1976**, *98*, 4853–4858.
- (2) Van Houten, J.; Watts, R. J. *Inorg. Chem.* **1978**, *17*, 3381–3385.
- (3) Durham, B.; Caspar, J. V.; Nagle, J. K.; Meyer, T. J. *J. Am. Chem. Soc.* **1982**, *104*, 4803–4810.
- (4) Allen, G. H.; White, R. P.; Rillema, D. P.; Meyer, T. J. *J. Am. Chem. Soc.* **1984**, *106*, 2613–2620.
- (5) Bhasikuttan, A. C.; Suzuki, M.; Nakashima, S.; Okada, T. *J. Am. Chem. Soc.* **2002**, *124*, 8398–8405.
- (6) Cannizzo, A.; van Mourik, F.; Gawelda, W.; Zgrablic, G.; Bressler, C.; Chergui, M. *Angew. Chem., Int. Ed.* **2006**, *45*, 3174–3176.
- (7) Hoff, D. A.; Silva, R.; Rego, L. G. C. *J. Phys. Chem. C* **2011**, *115*, 15617–15626.
- (8) Friedman, A. E.; Chambron, J. C.; Sauvage, J. P.; Turro, N. J.; Barton, J. K. *J. Am. Chem. Soc.* **1990**, *112*, 4960–4962.
- (9) Olson, E. J. C.; Hu, D.; Hörmann, A.; Jonkman, A. M.; Arkin, M. R.; Stemp, E. D. A.; Barton, J. K.; Barbara, P. F. *J. Am. Chem. Soc.* **1997**, *119*, 11458–11467.
- (10) Coates, C. G.; Olofsson, J.; Coletti, M.; McGarvey, J. J.; Önfelt, B.; Lincoln, P.; Norden, B.; Tuite, E.; Matousek, P.; Parker, A. W. *J. Phys. Chem. B* **2001**, *105*, 12653–12664.
- (11) Olofsson, J.; Önfelt, B.; Lincoln, P. *J. Phys. Chem. A* **2004**, *108*, 4391–4398.
- (12) Moucheron, C.; Kirsch-De Mesmaeker, A.; Choua, S. *Inorg. Chem.* **1997**, *36*, 584–592.
- (13) Masschelein, A.; Jacquet, L.; Kirsch-De Mesmaeker, A.; Nasielski, J. *Inorg. Chem.* **1990**, *29*, 855–860.
- (14) Kirsch-De Mesmaeker, A.; Jacquet, L.; Nasielski, J. *Inorg. Chem.* **1988**, *27*, 4451–4458.
- (15) Marcéls, L.; Ghesquière, J.; Garnir, K.; Kirsch-De Mesmaeker, A.; Moucheron, C. *Coord. Chem. Rev.* **2012**, *256*, 1569–1582.
- (16) Marcéls, L.; Moucheron, C.; Kirsch-De Mesmaeker, A. *Philos. Trans. R. Soc. A* **2013**, *371*, 20120131 (DOI: 10.1098/rsta.2012.0131).
- (17) Mattiuzzi, A.; Marcéls, L.; Jabin, I.; Moucheron, C.; Kirsch-De Mesmaeker, A. *Inorg. Chem.* **2013**, *52*, 11228–11236.
- (18) Nimse, S. B.; Kim, T. *Chem. Soc. Rev.* **2013**, *42*, 366–386.
- (19) Arduin, A.; Pochini, A.; Secchi, A.; Ugozzoli, F. Recognition of Neutral Molecules. In *Calixarenes 2001*; Asfari, Z., Böhmer, V.,

Harrowfield, J., Vicens, J., Saadioui, M., Eds.; Springer: Dordrecht, The Netherlands: 2002; pp 457–475.

(20) Kim, S.; Kim, H.; Yoon, J.; Kim, J. Fluorescent Chemosensors. In *Calixarenes in the Nanoworld*, Vicens, J., Harrowfield, J., Baklouti, L., Eds.; Springer: Dordrecht, The Netherlands: 2007; pp 311–333.

(21) Coquiere, D.; Le Gac, S.; Darbost, U.; Seneque, O.; Jabin, I.; Reinaud, O. *Org. Biomol. Chem.* **2009**, *7*, 2485–2500.

(22) Menand, M.; Jabin, I. *Org. Lett.* **2009**, *11*, 673–676.

(23) Cornut, D.; Marrot, J.; Wouters, J.; Jabin, I. *Org. Biomol. Chem.* **2011**, *9*, 6373–6384.

(24) Moerkerke, S.; Ménand, M.; Jabin, I. *Chem.—Eur. J.* **2010**, *16*, 11712–11719.

(25) Menand, M.; Jabin, I. *Chem.—Eur. J.* **2010**, *16*, 2159–2169.

(26) Silvi, S.; Arduini, A.; Pochini, A.; Secchi, A.; Tomasulo, M.; Raymo, F. M.; Baroncini, M.; Credi, A. *J. Am. Chem. Soc.* **2007**, *129*, 13378–13379.

(27) Pappalardo, S.; Villari, V.; Slovak, S.; Cohen, Y.; Gattuso, G.; Notti, A.; Pappalardo, A.; Pisagatti, I.; Parisi, M. R. *Chem.—Eur. J.* **2007**, *13*, 8164–8173.

(28) Darbost, U.; Rager, M.-N.; Petit, S.; Jabin, I.; Reinaud, O. *J. Am. Chem. Soc.* **2005**, *127*, 8517–8525.

(29) Herman, L.; Elias, B.; Pierard, F.; Moucheron, C.; Kirsch-De Mesmaeker, A. *J. Phys. Chem. A* **2007**, *111*, 9756–9763.

(30) Deroo, S.; Le Gac, S.; Ghosh, S.; Villien, M.; Gerbaux, P.; Defrancq, E.; Moucheron, C.; Dumy, P.; Kirsch-De Mesmaeker, A. *Eur. J. Inorg. Chem.* **2009**, *2009*, 524–532.

(31) Kirsch-De Mesmaeker, A.; Nasielski-Hinkens, R.; Maetens, D.; Pauwels, D.; Nasielski, J. *Inorg. Chem.* **1984**, *23*, 377–379.

(32) Lecomte, J. P.; Kirsch-De Mesmaeker, A.; Demeunynck, M.; Lhomme, J. J. *Chem. Soc., Faraday Trans.* **1993**, *89*, 3261–3269.

(33) The real values of the quenching constants k_q should probably correspond to higher values since the calixarene is protonated only to 86%. Moreover, it should be noted that nonprotonated **1** in MeCN , but not in BuCN , quenches the excited complex by 20%–25% (from ± 1800 ns to 1400 ns under Ar with 1 mM of **1**). This is due to the amine electron donor group of **1**. However, this effect is negligible versus the quenching by $\mathbf{1}^{\bullet\text{H}^+}$.

(34) The emission lifetime of $[\text{Ru}(\text{TAP})_2\text{phen}]\text{Cl}_2$ in BuCN depends also on the complex concentration due to Cl^- .

(35) Lakowicz, J. R. *Principles of Fluorescence Spectroscopy*; Springer: London, 2009.

(36) Marton, A.; Clark, C. C.; Srinivasan, R.; Freundlich, R. E.; Sarjeant, A. A. N.; Meyer, G. J. *Inorg. Chem.* **2006**, *45*, 362–369.

(37) Ward, W. M.; Farnum, B. H.; Siegler, M.; Meyer, G. J. *J. Phys. Chem. A* **2013**, *117*, 8883–8894.

(38) The exergonicity is evaluated by the equation $\Delta G^0 = -nF[E_{\text{red}}^*(\text{Ru}^{\text{II}}/\text{Ru}^{\text{I}}) - E_{\text{ox}}(\text{Cl}^-/\text{Cl}^{\bullet})]$, where $E_{\text{red}}^*(\text{Ru}^{\text{II}}/\text{Ru}^{\text{I}}) = +1.06$ V vs SCE^{15} and $E_{\text{ox}}(\text{Cl}^-/\text{Cl}^{\bullet}) = +1.05$ V vs SCE^{45} .

(39) This signal is difficult to observe, because it lies more or less in the same spectral region as the absorption of the $^3\text{MLCT}$ state.

(40) Meyer, T. J. *Pure Appl. Chem.* **1986**, *58*, 1193–1206.

(41) Kober, E. M.; Sullivan, B. P.; Meyer, T. J. *Inorg. Chem.* **1984**, *23*, 2098–2104.

(42) Boisdenghien, A. Photophysique et photochimie de complexes de $\text{Ru}(\text{II})$ en présence d'acides nucléiques, d'amines aminés et des biopolymères correspondants. Ph.D. Thesis, Université Libre de Bruxelles, Brussels, Belgium, 2007.

(43) Kirsch-De Mesmaeker, A.; Maetens, D.; Nasielski-Hinkens, R. J. *Electroanal. Chem.* **1985**, *182*, 123–132.

(44) Alary, F.; Boggio-Pasqua, M.; Heully, J.-L.; Marsden, C. J.; Vicendo, P. *Inorg. Chem.* **2008**, *47*, 5259–5266.

(45) Harrison, J. A.; Hermijanto, S. D. *J. Electroanal. Chem.* **1987**, *225*, 159–175.